THE ASTRONOMICAL JOURNAL VOLUME 106, NUMBER 1 JULY 1993

# SPECTRAL-LINE BROADENING FUNCTIONS OF W UMa-TYPE BINARIES. II. AH Vir

W. -X. LU AND S. M. RUCINSKI

Institute for Space and Terrestrial Science and Department of Physics and Astronomy, York University, 4700 Keele Street, Toronto, Ontario M3J 1P3, Canada

Electronic mail: rucinski@dorado.sal.ists.ca

*Received 1993 March 3; revised 1993 March 29*

## ABSTRACT

Twenty-four 10 Å/mm spectra of the W UMa binary AH Vir have been analyzed for radial velocities and for geometrical parameters of the system components by the method of spectral-line broadening functions. It is shown that the broadening functions determined through the linear restoration process are much better defined than cross-correlation functions, even in the presence of broad spectral features. A new spectroscopic orbit for AH Vir has been determined on the basis of radial velocity information contained in the broadening functions. A combination of this orbit with a parallel solution for the geometric elements gave a new set of absolute elements of the system: $a=2.80R_{\odot}$, $M_1=1.36M_{\odot}$, $M_2=0.41M_{\odot}$, $R_1=1.40R_{\odot}$, and $R_2=0.83R_{\odot}$. The absolute bolometric magnitude of the system was found to be $4^{m}07$ and the distance about 94 pc. AH Vir belongs to the OO Aql subclass of contact binaries which is characterized by the unusually low effective temperature for the observed large dimensions. The radius of the primary (more massive component) is close to what would be expected if it obeyed the Main-Sequence mass–radius relation, but the luminosity of the system (most likely produced solely by the primary component) is lower than that for the Zero-Age Main Sequence. The underluminosity of the system is due to the abnormally low effective temperature which remains significantly low after the energy transfer between components is taken into account. We speculate that the unusual properties of AH Vir result from lack of thermal equilibrium related to the mass transfer between components.

## 1. INTRODUCTION

The W UMa-type binary AH Vir (HD 106400, SAO 100003, BD+12°2437, ADS 8472A; $P=0.408$ day, $B-V=0.76$; the companion ADS 8472B of $13^{m}2$ is at 1".3 separation) was discovered as a variable star by Guthnick & Prager (1929). The binary is among the most active contact systems, and is one of the few W UMa-type variables whose occultation eclipses are total. Therefore, since its discovery, many investigations have been devoted to the determination of the system parameters, mostly geometric ones based on the photometric data. The first spectroscopic orbit was determined by Chang (1948), who obtained 31 spectra of which 9 showed the radial velocities of the secondary component. Because of the low dispersion (76 Å/mm at Hγ), the necessity of long exposure times, and the difficulty in velocity measurements based on severely blended spectra using the classical methods, Chang's data showed large scatter. In fact, these measurements are inadequate by modern standards but most of the subsequent photometric solutions utilized Chang's value of the mass ratio, $q=0.42$, because no other value was available (Binnendijk 1960; Lucy 1973; Niarchos 1983). Recognizing the uncertainty in $q$, Hilditch (1981), Jabbar & Kopal (1983), Kaluzny (1984), and Binnendijk (1984) made photometric solutions by adjusting the mass ratio, but each investigation led to a different set of final parameters. Thus, the inclination $i$ was found to range between 71° and 88° and the mass-ratio $q$ between 0.26 and 0.44. The degree of contact was also poorly determined. In fact, the spread in solutions was so large that the resultant configurations ranged from those of slight detachment to overcontact exceeding 40%. This large spread in the results illustrates difficulties encountered in light curve solutions performed without a well determined mass ratio, even for totally eclipsing systems such as AH Vir.

Barden (1984, 1985) attempted a new determination of a spectroscopic orbit and found a mass ratio of 0.34. He also claimed to be able to measure the velocity of the visual companion ADS 8472B. However, with only 11 observations in total and the poor phase coverage, Barden's determination of $q$ remained tentative.

AH Virginis is a particularly important contact system for two reasons. One reason is its evolutionary state. As was shown by Mochnacki (1981), AH Vir belongs to the group of cool contact systems which are too large and have periods too long to have been always in contact. These systems, called the OO Aql group, probably resulted from mergers of slightly evolved, detached binary systems. While this conclusion is primarily derived from the long period for the observed late spectral type, the mass ratio is also important as it determines the relative sizes of components. The other reason is the strong activity of AH Vir observed in Hα (Barden 1985) and in Mg II (Rucinski 1985), and its strongly variable light curve (Binnendijk 1960, 1984; Bakos 1977) which always retains the W-type characteristics of the deeper occultation minima (Rucinski 1974). Most of these indicators point to the more massive component as being much more active than the smaller secondary. Barden's Hα observations were particularly in-

 0004-6256/93/106(1)/361/11/$0.90  

TABLE 1. Radial-velocity observations of AH Vir derived from Gaussian fits.

| H.J.D 2,400,000+ | Phase† | star 1 | | | | star 2 | | | |
|---|---|---|---|---|---|---|---|---|---|
| | | $RV_b$ | $(O-C)_b$ | $RV_c$ | $(O-C)_c$ | $RV_b$ | $(O-C)_b$ | $RV_c$ | $(O-C)_c$ |
| 48764.574 | 0.197 | 80.7 | −3.9 | 71.3 | −3.2 | −246.1 | −6.2 | −243.8 | −7.8 |
| 48764.587 | 0.231 | 82.0 | −6.3 | 79.7 | 1.7 | −255.4 | −3.1 | −249.5 | −0.2 |
| 48764.597 | 0.254 | 84.7 | −4.2 | 70.6 | −8.0 | −257.7 | −3.6 | −258.9 | −7.2 |
| 48764.604 | 0.273 | 87.9 | −0.2 | 82.2 | 4.3 | −246.3 | 5.2 | −241.4 | 8.2 |
| 48764.614 | 0.298 | 80.7 | −4.7 | 77.5 | 1.6 | −239.7 | 2.8 | −231.9 | 9.4 |
| 48764.622 | 0.316 | 83.9 | 1.7 | 75.7 | 2.4 | −223.5 | 8.5 | −217.6 | 13.8 |
| 48764.632 | 0.341 | 73.7 | −2.7 | 69.0 | 0.6 | −209.2 | 3.4 | −206.4 | 6.4 |
| 48764.639 | 0.358 | 73.3 | 2.1 | 64.0 | 3.1 | −196.1 | −0.6 | −193.4 | 2.9 |
| 48764.649 | 0.383 | 69.7 | 7.1 | 64.6 | 7.9 | −163.9 | 3.1 | −164.8 | 3.7 |
| 48764.657 | 0.401 | 67.5 | 12.0 | 45.4 | −5.3 | −133.6 | 10.0 | −152.9 | −7.3 |
| 48765.575 | 0.656 | −64.1 | −7.4 | −55.3 | −8.5 | 231.5 | 3.5 | 230.7 | 6.6 |
| 48765.583 | 0.674 | −62.7 | −1.4 | −53.4 | −2.4 | 248.6 | 5.3 | 248.5 | 8.7 |
| 48765.592 | 0.697 | −67.6 | −1.7 | −60.4 | −5.3 | 258.1 | −0.4 | 254.9 | −0.5 |
| 48765.601 | 0.718 | −77.8 | −9.1 | −63.1 | −5.5 | 262.1 | −5.6 | 258.3 | −6.7 |
| 48765.610 | 0.742 | −71.8 | −1.7 | −63.0 | −3.9 | 264.5 | −8.0 | 261.5 | −9.0 |
| 48765.618 | 0.760 | −73.4 | −3.3 | −61.2 | −2.0 | 255.8 | −16.6 | 255.8 | −15.0 |
| 48765.629 | 0.787 | −63.3 | 4.8 | −52.6 | 5.1 | 260.4 | −5.5 | 258.4 | −6.8 |
| 48765.636 | 0.804 | −63.4 | 2.2 | −54.8 | 0.8 | 268.9 | 11.2 | 265.3 | 7.8 |
| 48765.645 | 0.827 | −64.5 | −3.5 | −52.6 | −0.8 | 238.5 | −3.9 | 236.9 | −6.0 |
| 48765.653 | 0.846 | −49.0 | 7.1 | −40.8 | 6.8 | 226.6 | 0.7 | 229.4 | 2.3 |
| 48765.663 | 0.870 | −59.0 | −10.3 | −50.9 | −9.6 | 192.9 | −8.5 | 197.7 | −5.6 |
| 48765.671 | 0.890 | −48.7 | −7.5 | −36.1 | −1.1 | 178.7 | 1.8 | 191.0 | 11.7 |
| 48765.680 | 0.912 | −24.5 | 8.1 | −23.4 | 4.2 | 176.3 | 28.2 | 177.0 | 25.9 |
| 48788.590* | 0.128 | 64.2 | −2.5 | 49.8 | −8.8 | −185.0 | −4.2 | −186.0 | −10.2 |

Comments:

The subscripts b and c represent the radial-velocity measurements from the BF and CCF, respectively.

† Values of phases for the CCF results have been reduced by $0^p.002$ ( see text).

* Blue spectrum centered at the G-band.

teresting as they revealed emission from the primary and absorption from the secondary. Mullan (1975) conjectured that the marginal contact observed in W UMa-type systems results in differential susceptibility of the components to spot formation with the more massive primary having a tendency to produce larger spots. The same tendency for stronger activity of the primary component can be explained by the observation that, for common envelopes of constant entropy, the primary components are *expected* to have relatively deeper convective envelopes (Rucinski 1992a) because of the differential mass–radius relation imposed by the contact geometry.

In this study, we present a spectroscopic orbit for AH Vir based on our radial-velocity measurements, processed using the newly developed method of Broadening Functions (hereafter referred to as BF; Rucinski 1992b=Paper I). The spectroscopic observations and reductions are described in Secs. 2 and 3. The new spectroscopic orbit obtained from the traditional analysis of the spectroscopic data is presented in Sec. 4. Section 5 presents determinations of additional contact-model parameters on the basis of the literature light curves and the new BF's. The absolute orbital parameters of AH Vir are discussed in Sec. 6. Section 7 gives a short rediscussion of the spatial velocity of the system on the basis of the new distance determination. The last, Sec. 8, gives a summary and conclusions of the paper.

## 2. OBSERVATIONS

The binary AH Vir was observed on the nights of 1992 May 21 and 22 and June 14, at David Dunlap Observatory. A total of 24 spectra were obtained with the 1.88 m telescope and the Cassegrain spectrograph giving a dispersion of 10 Å/mm. The 1024×1024 pixel CCD detector covered a wavelength interval of about 210 Å in the yellow part of the spectrum around 5000 Å with a spectral resolution of 0.21 Å/pixel. The exposure times were kept equal to 10 min with corresponding resolution in orbital phase of $0^p.017$. The signal-to-noise ratios (S/N) ranged between 30 to 60 due to the variable weather conditions. A journal of observations is presented in Table 1. The heliocentric Julian Dates denote the midpoints of exposures. The phases were computed following the photometric conven-

tion of the origin at the deeper eclipse (this origin has been redetermined, as described in Sec. 4). Following another convention, the suffix "1" in Table 1 and throughout the paper represents the more-massive, more-luminous, but slightly cooler star eclipsed at the secondary (shallower) minimum ($0^P5$). For calibration of radial velocities, we utilized five standard stars taken from *Astronomical Almanac 1992* pages H42–43, of which HD 102870 (F9V) and HD 171232 (G8III) served also as templates for the BF determinations.

One blue spectrum of AH Vir obtained on June 14 was centered at the G band. This spectrum permitted an estimate of the spectral type of AH Vir on the basis of relative strengths of spectral features such as $\lambda\lambda$ 4216, 4227, 4326, and 4340. Given the strong blending of the spectral features, our estimate, about G8V, is in a good agreement with the other classifications: K0V (Chang 1948), K0n and K0III (Hill *et al.* 1975), G8IV (Hilditch 1981), and G9V (Barden 1985). This late spectral type led to some difficulty with the BF derivation as the principal template (HD 102870, F9V) did not match the spectrum of AH Vir very well (see next section).

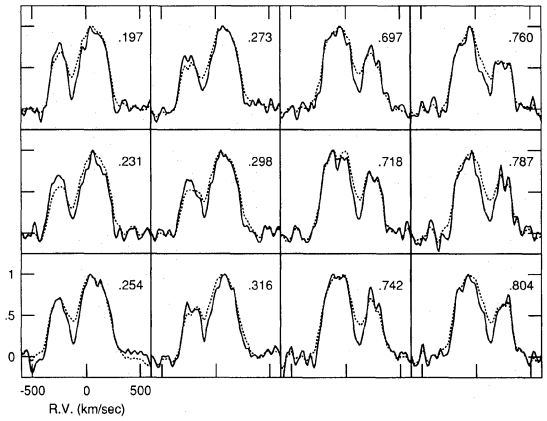


FIG. 1. A comparison of BF (solid) and CCF (dashed) profiles for spectra obtained around the orbital quadratures. They were calculated using the same template spectrum of HD 102870. Note that the BF's have much higher resolution than the CCF's because the natural broadening of lines in the template is subtracted rather than added to the final result. The orbital phases are given within each panel.

## 3. DATA REDUCTION

The data reductions were performed in the following way. First, the two-dimensional CCD images were converted into one-dimensional (1D) spectra within IRAF.[1] A number of IRAF subroutines were used to remove the bias and to perform the flat-fielding, cosmic-ray removal, 1D extraction, wavelength calibration, and rectification. Then the spectra were reduced further within the software system IDL by means of programs permitting determination of the BF, as described for the case of AW UMa in Paper I. The broadening function is a description of strictly geometric line-broadening effects and is derived assuming that the local intensity spectra are identical with the flux spectra of preselected, slowly rotating (template) stars. The BF determination involves rebinning the spectra to equal velocity steps and a least-squares solution utilizing the Singular Value Decomposition to remove linear dependencies resulting from presence of the featureless spectral continuum. The BF's thus obtained contain high frequency noise which can be easily removed by a Gaussian profile smoothing. The one-sigma width of this smoothing was set to 9.6 km/s.

We could obtain two sets of the BF profiles using two sharp-line standards HD 102870 ($\beta$ Vir, $V \sin i = 3$ km/s, F9V) and HD 171232 (G8III) as templates. Because the S/N for HD 102870 was much higher ($\sim$250) than for HD 171232 ($\sim$100), the BF determinations based on the former template had a much higher quality in spite of the poor match in spectral types: about G8V for AH Vir versus F9V for HD 102870. This mismatch had no practical consequences for determinations of the radial velocities of components but was a complicating factor for determinations of system parameters such as the degree-of-contact or the temperature excess of the secondary component, as these quantities are derived primarily from *shapes* of the BF's.

In addition to the BF profiles, we also calculated cross-

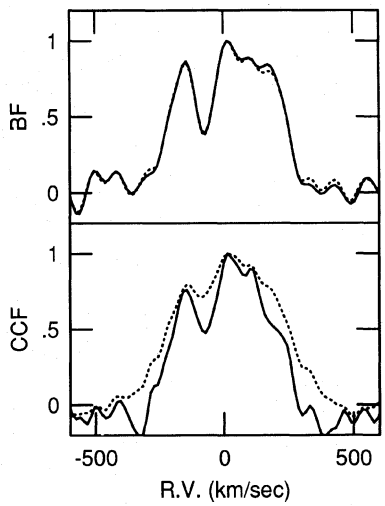


FIG. 2. This figure demonstrates that the BF approach has a great advantage over the CCF technique. The BF (upper panel) and CCF (lower panel) profiles were obtained for the blue spectrum of AH Vir centered at the G band. The solid curves in each panel were computed by excluding the G band, while the dashed ones were calculated with the presence of the G band. It is clearly seen that the BF profiles are less dependent than the CCF on the presence or exclusion of the broad features.

[1]IRAF is distributed by the National Optical Astronomy Observatories, which is operated by the Association of Universities for Research in Astronomy, Inc., under contract to the National Science Foundation.

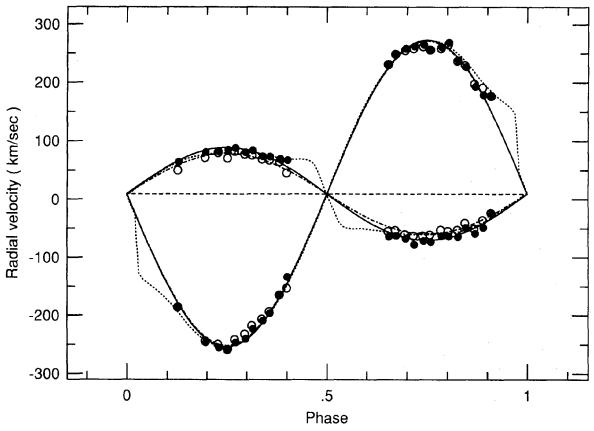


FIG. 3. Radial–velocity curves of AH Vir. The filled and open circles give radial–velocity measurements obtained by fitting double Gaussians to the BF and CCF profiles, respectively. The solid and dot–dash curves were obtained for the BF and CCF data under the assumption that the stellar components are free from photometric distortions and revolve on circular orbits. The dotted lines give the fit computed for the BF data with corrections for the Roche model obtained with the Wilson–Devinney code. A separate solution, which cannot be shown here, but which we adopted, involved a simple shift and scale fit of the theoretical BF's to the observational results (see the text). It has a great advantage of being independent of the dubious assumption about the Gaussian (or similar) shape of the components in the spectral domain.

correlation function (CCF) profiles for all rebinned spectra against the same template spectrum of HD 102870. CCF profiles have been used by many researchers analyzing W UMa stars as a means of extracting the velocity and component shape information from high resolution spectra. As expected, the CCF results are inferior to the BF results in terms of resolution and overall quality. For comparison, we show in Fig. 1 the BF (solid curves) and CCF (broken lines) profiles for the subset of our spectra which were obtained around the orbital quadratures. It is clear that all the BF profiles have higher resolution than their CCF counterparts. A closer scrutiny reveals systematic differences in the "neck" area between the peaks which has a direct bearing on the degree-of-contact determination for AH Vir.

The inferior quality of the CCF profiles and their dependence on the intrinsic broadening in the sharp-line spectrum are particularly evident in Fig. 2, which shows a comparison of the BF and CCF profiles derived from the same (and only) blue spectrum of AH Vir, using the same standard star and the same wavelength region. The upper panel shows the BF result and the lower panel shows the CCF result. The solid lines in each panel give profiles obtained excluding the G band (which is the broadest feature in this region) whereas the dashed lines give the results with the G band included. As we see, the BF result is independent of the presence or exclusion of the G band, but the CCF result is crucially dependent on the presence of the G band. This example clearly illustrates the great advantage of the BF approach over the CCF approach. The BF method does not call for any removal of broad features. In fact, this would be disadvantageous as it would only lower the information content in spectra and lower accuracy of the final result. We note that our spectra are free from any broad features but we stress that we no longer need to avoid them if we use the BF approach.

The orbital solutions presented in this paper were obtained using two independent approaches. The first, more traditional approach was through representation of the BF and CCF profiles by two Gaussians. As we discuss in Sec. 4, these measurements were used twice for the spectroscopic orbit: directly, i.e., without corrections for the non-Gaussian shape of the actual profiles, and with corrections from the Wilson–Devinney model. The second approach described in Secs. 5 and 6, did not give individual radial velocities but was much more precise for the velocity amplitude determination. It involved fits of the theoretical BF's (calculated with a light synthesis model) to the observed profiles, without splitting them into individual components.

Our velocity measurements were relative to HD 102870 whose velocity, as well as the velocities of the other standards, were taken from the *Astronomical Almanac 1992*. The measurements for this star were checked for consistency by measurements of the other four standards with agreement to $0.3 \pm 0.8$ km/s. The results of the Gaussian fits to the two components of AH Vir are tabulated in Table 1 and shown graphically in Fig. 3, together with the orbital solutions discussed in the next section. The (O–C) values listed in the table are for the circular orbit and are indicative of the quality of our observations. We did not use the circular orbit solution for the final element determination, but based it entirely on the $K_1+K_2$ scaling of global BF fits, as described in Secs. 4–6.

We can see in Fig. 3 that the measurements by the cross-correlation technique noticeably underestimated the velocity amplitude of the more massive star but also slightly underestimated the amplitude of the secondary star because the two stellar lines blended together biasing the peak of the CCF toward small velocities.[2] As most modern mass determinations for W UMa systems are obtained by the CCF method, we call attention to this systematic discrepancy, which should be checked for other systems. The remaining discussion will be based on the results derived solely from the broadening functions.

We note that the visual component of AH Vir (ADS 8472B) could not be detected in the profiles derived from either (BF or CCF) method. This is not unexpected as this component is over 40 times fainter than AH Vir. The Barden (1984, 1985) spectroscopic detection of the visual companion may have benefited from the longer wavelengths at which he observed (the H$\alpha$ region), because the spectral type of the tertiary was estimated by him to be K5V. An inspection of his results indicates a very large scatter in velocities of ADS 8478B, suggesting that the measurements were difficult and possibly unreliable.

[2]It should be noted that the apparent underluminosity of AH Vir that we discuss later on, is still present if we use the CCF result in place of our final solution based on the BF profiles.

TABLE 2. Spectroscopic orbital elements of AH Vir.

| element | BF circ. | CCF circ. | BF WD model | BF direct fit |
|---|---|---|---|---|
| $V_0$ (km s$^{-1}$) | $+9.3 \pm 1.2$ | $+9.7 \pm 1.3$ | $+6.6 \pm 0.9$ | $+8.1 \pm 0.8$ |
| $K_1$ (km s$^{-1}$) | $79.6 \pm 1.6$ | $68.9 \pm 1.7$ | $80.7 \pm 0.6$ | $80.5 \pm 1.3$ |
| $K_2$ (km s$^{-1}$) | $263.5 \pm 1.9$ | $261.4 \pm 2.0$ | $266.3 \pm 2.0$ | $265.6 \pm 1.7$ |
| $\Delta\phi_0$† | $0^p.000 \pm 0^p.002$ | $0^p.002 \pm 0^p.002$ | $0^p.006 \pm 0^p.002$ | $0.0$‡ |
| $q$ $(m_2/m_1)$ | $0.302 \pm 0.006$ | $0.264 \pm 0.007$ | $0.303 \pm 0.006$ | $0.303$‡ |
| $a_1 \sin i$ $(R_\odot)$ | $0.641 \pm 0.013$ | $0.555 \pm 0.013$ | $0.650 \pm 0.005$ | $0.648 \pm 0.010$ |
| $a_2 \sin i$ $(R_\odot)$ | $2.122 \pm 0.015$ | $2.105 \pm 0.016$ | $2.144 \pm 0.016$ | $2.139 \pm 0.014$ |
| $m_1 \sin^3 i$ $(M_\odot)$ | $1.312 \pm 0.021$ | $1.206 \pm 0.021$ | $1.357 \pm 0.021$ | $1.346 \pm 0.024$ |
| $m_2 \sin^3 i$ $(M_\odot)$ | $0.396 \pm 0.010$ | $0.318 \pm 0.009$ | $0.411 \pm 0.007$ | $0.408 \pm 0.010$ |
| $s.d.$* (km s$^{-1}$) | $\pm 7.3$ | $\pm 7.6$ | $\pm 6.0$ | – |

Comments:

† $\Delta\phi_0$ is the phase shift.

‡ Assumed.

* Standard deviation of unit weight for the solution.

## 4. SPECTROSCOPIC ORBIT

This section describes a more traditional approach in which the BF and CCF profiles are assumed to be composed of two separate components. This approach does not extract from the profiles any information on the degree of contact or on the deviations of the surface brightness distribution from the strict contact model but allows us to determine the mass ratio which can be subsequently used in global BF fits. In brief summary, our approach was as follows. After determining the value of the mass ratio using the traditional analysis described below, we redetermined the geometric elements of the system from the light curves and the BF's by *assuming* the new value of the mass ratio. With these elements, we obtained a new solution for the spectroscopic scale of the system, $K_1+K_2$, by fitting the observed BF's with model profiles computed with a light-synthesis code (Secs. 5 and 6).

Three sets of orbital elements were obtained from the separate solutions of the velocities from the BF and CCF profiles using the traditional approach. They are listed in Table 2. First, we used a Gaussian fit to the component profiles and then solved the spectroscopic orbit using a simple circular orbit. The least-squares problem RVORBIT (Hill 1991) was used for the orbit solution. Equal weights were assigned to all radial velocities. As the program finds the time $T$ of the positive maximum velocity of the primary star, we added one quarter of the period to obtain the photometric initial epoch $T_0$. The period was set equal to the recently derived value of $0^d.40752779$ (Demircan *et al.* 1991). Two solutions based on the BF and CCF profiles with Gaussian fittings are listed in the first two columns of Table 2. We found that our determination of the initial epoch, $T_0$, differed slightly from the most recent time of light minimum HJD 2447569.6214 (Demircan *et al.* 1991) for the BF and CCF solutions (the line $\Delta\phi_0$ in Table 2).

The next solution listed in the third column of Table 2 is based on the velocity data corrected for the proximity and eclipse light-centroid effects, which were calculated using the Wilson–Devinney program (WD; Wilson 1979). The definition of the centroid corrections was given in Wilson & Sofia (1976).

The three solutions discussed above were aimed at a determination of a reliable value of the mass ratio $q$, to be used in the subsequent analysis. The fourth column in Table 2 gives one more solution obtained with the *assumed* $q=0.303$. This solution utilized scaling of the theoretical BF's by a common factor $K_1+K_2$, and shifting by $V_0$, in a way similar to that used in Paper I for AW UMa. This solution required knowledge of the additional geometric parameters of the system and was performed after the analysis described in the next section.

In discussing the solutions in Table 2 which were based on the double-Gaussian fits, we would like to emphasize that the velocity amplitudes and the mass ratio derived from the BF's are significantly different from those from the CCF. The differences in $K_1$ and in $q$ are particularly significant. This is shown in Fig. 3 where the solutions given in the first three columns of Table 2 are graphically compared. We note that the velocity amplitudes are only slightly changed when we correct radial velocities derived from the BF's for the line-centroid shifts using the WD program. The WD corrections did not influence the mass ratio of the system, which remained very close to that derived from sinusoidal fits to the radial velocities. Anticipating results of the fourth and final solution, to be discussed in Sec. 6, we note that the parameters obtained by "horizontal" shifts and stretching of the theoretical broadening functions gave values of $V_0$ and $K_1+K_2$ very close to those for the solution based on data obtained by Gaussian fitting with the light-centroid WD corrections.

TABLE 3. Geometrical parameters of AH Vir.

| element | V | B | BF HD102870(F9V) | BF HD171232(G8III) |
|---|---|---|---|---|
| $i$ | 85°.2 ± 1°.2 | | – | – |
| $f$ | 0.206 ± 0.021 | | 0.270 ± 0.036 | *fixed* |
| $X$ | 0.092 ± 0.012 | 0.069 ± 0.008 | 0.069 ± 0.006 | 0.063 ± 0.007 |

Comments:
Assumed $q = 0.303$.
Columns V and B: parameters derived from the light curves of Binnendijk(1960).
Columns BF: parameters derived from Broadening Functions.

Irrespective of the type of solution, the value of the systemic velocity, $V_0$, is in very good agreement with that given by Chang (1948). However, the amplitudes $K_1$ and $K_2$ and the derived mass ratio are quite different from those of Chang ($K_1=105$ km/s, $K_2=250$ km/s, $q=0.42$). Since the radial velocities in the present study are based on many more spectra of much better quality which were measured using modern methods, we feel that the new orbit is preferred. The mass ratio derived by us ($q=0.30$) is also different from that of Barden (1984, 1985; $q=0.34$), and is better determined because we have more observations and good phase coverage of velocity curves.

## 5. THE CONTACT-MODEL PARAMETERS OF AH VIRGINIS

Our new spectroscopic data are of sufficiently good quality to motivate rediscussion of the absolute parameters of AH Vir. We felt that a new analysis of the contact model geometric elements of the system was warranted at this stage. We have done so twice, on the basis of the literature light curves and our new BF profiles, as described in the two subsections below.

### *5.1 Solutions of the V and B light curves for i, f, and X*

Several light curves of AH Vir have been described in the literature [Binnendijk 1960, Bakos 1977; Hilditch 1981 (unpublished); Demircan *et al.* 1991 (unpublished)]. Most of these curves show strong variability which may be associated with spot formation on one or both components. With our new value of the spectroscopic mass ratio, we attempted a new light curve synthesis solution for AH Vir. We used Binnendijk's (1960) observations obtained on 1957 May 1, 2, 3 [the same as used by Kaluzny (1984)] and formed 56 normal points for each of the two, $V$ and $B$, light curves. These light curves look symmetric and seem to be relatively unperturbed. There is a $13^{m}.2$ companion in the system (Binnendijk 1960) which contributes 2.3% and 1.6% to the total systemic light in the $V$ and $B$ bands, respectively, adopting Barden's (1985) classification of K5V of the companion. The companion is only 1".3 away from the eclipsing pair and its photometric parameters are poorly known. We note that Kaluzny (1984), who elected to determine the third light contribution from the light curve solutions, obtained somewhat larger values of 7.6% in $V$ band and 6.5% in $B$ band. We also attempted to determine this contribution but found that its inclusion destabilizes the light curve synthetic solutions. Therefore, we fixed the level of the third light at 2.3% in $V$ and 1.6% in $B$ and simply subtracted them from the light curves. These corrections have very small influence on the final solutions.

Following the widespread conventions in the field of photometric solutions of W UMa-type systems, we assumed the gravity darkening exponent $g$ to be 0.08 (Lucy 1967) and fixed the bolometric albedo $A$ at 0.5 (Rucinski 1969). The limb-darkening coefficients $u$ were interpolated from the table of Al-Naimiy (1978). The effective temperature $T_1$ of the primary was fixed at 5300 K according to its spectral type of G8V using the calibration of Popper (1980). The mass ratio $q=\mathcal{M}_2/\mathcal{M}_1$ was fixed at the spectroscopic value from the solution based on the BF results, as in Sec. 4. The theoretical light curves and broadening functions were computed using the same synthesis program as that used for AW UMa (Paper I; also Rucinski 1976a). The geometric parameters of the system: the orbital inclination, $i$, the degree of contact, $f$, and the relative

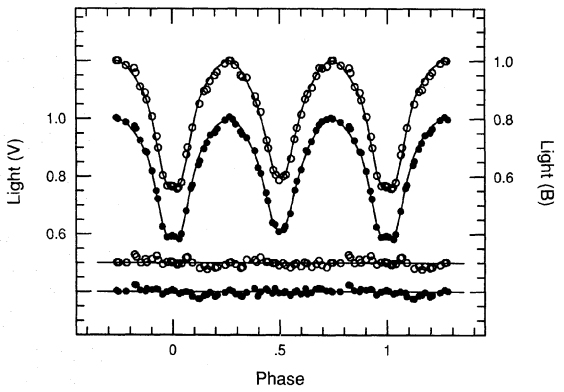


FIG. 4. The Binnendijk (1960) light curves of AH Vir in $B$ (open circles) and in $V$ (filled circles) together with the light-curve-synthesis fits (solid curves) generated by our light-synthesis program. The corresponding residuals are shown in the lower part of the figure.

TABLE 4. A comparison of orbital elements of AH Vir.

| $i$ | $f$ | $X$ | $q$ | source |
|---|---|---|---|---|
| $81.0 \pm 1.6$ | $0.25 \pm 0.02$ | $0.032 \pm 0.016$ | $0.33 \pm 0.03$ | Hilditch(1981)* |
| $84.1 \pm 0.5$ | $0.158 \pm 0.016$ | – | $0.318 \pm 0.005$ | Binnendijk(1984) |
| $86.5 \pm 1.5$ | $0.238 \pm 0.026$ | $0.071 \pm 0.003$ | $0.342 \pm 0.016$ | Kaluzny(1984) |
| $85.2 \pm 1.2$ | $0.230 \pm 0.029$ | $0.070 \pm 0.008$ | $0.303 \pm 0.006$ | Present paper |

Comments:

* One of the six Hilditch (1981) solutions, which is the most similar to our solution in terms of the assumptions.

temperature excess of the secondary, $X$, were determined by a least-squares approach utilizing linearized equations for parameter corrections. We recall that the degree of contact is defined through the Jacobi equipotentials: $f=(C_1-C)/(C_1-C_2)$ ($f=0$ inner, $f=1$ outer contact), and the relative temperature excess is defined through the temperature excess of the secondary component, $X=\Delta T_s/T_s=(T'_s-T_s)/T_s$, where $T_s$ is the temperature expected from the unperturbed contact model and $T'_s$ is the actual temperature of the secondary (Rucinski 1974). (We will drop the subscript $s$ for clarity.) We use $X$ here for operational simplicity and stress that the optical data can be equally well described either by differential spot coverage or a difference in effective temperatures of components. However, the evidence from other wavelengths suggests that the former possibility is closer to the reality (Rucinski 1976b; Eaton *et al.* 1980).

The parameters found from the simultaneous solutions of the $V$ and $B$ light curves are listed in the second and third columns of Table 3 and the resulting theoretical light curves are shown in Fig. 4, together with the normal points formed from Binnendijk's observations. The present results are compared with the previous ones from the literature in Table 4. In this table, our values for $f$ and $X$ are the weighted averages of those presented in Table 3. The existing determinations agree reasonably well in general terms. We note, in particular, that the mass ratios determined photometrically by Binnendijk (1984) (the photometric $q=0.318$ and the "synthetic spectroscopic" $q_s=0.304$) were very close to our current spectroscopic determination. The new values of $(f, q, i)=0.23, 0.303, 85.2)$ predict—following the approach of Mochnacki & Daughty (1972)—that the eclipse totality should last about 35 min, whereas Binnendijk (1960) estimated this duration to be about 40 min, but no error estimate was attached to this value. The geometric contact in the orbital plane, $d_y$ (the half-thickness of the "neck" between stars), for the combination of $(f, q)$ as above, is $d_y=0.104\pm0.007$ in separation units. Thus, using $a$ as discussed in Sec. 6, the full geometric contact is $2d_y a=0.58\ R_\odot$. Thus, the small value of $f$ is somewhat misleading and the actual contact between stars is quite strong.

The temperature excesses $X=\Delta T/T$ determined by different authors, as listed in Table 4, do not agree. This could be expected, because $X$ has been used in place of the proper description of the differential spot coverage of the components and this could be different in different epochs. This important problem is outside the scope of the present paper. As we mentioned above, the simplest explanation of the W-type class of W UMa systems is in terms of star spots which preferentially form on the more massive component. Apparently, AH Vir always shows this differential effect whose magnitude varies but the sense (sign of $X$) remains always the same.

### 5.2 *Solutions of the BF Profiles for f and X*

Light curves of W-type systems depend basically on four parameters: the mass ratio, $q$, the inclination, $i$, the degree-of-contact, $f$, and the temperature excess, $X$. The broadening functions offer a substantial advantage over the light curves in the parameter dependence as they depend practically on only $q$, $f$, and $X$. With $q$ fixed from the

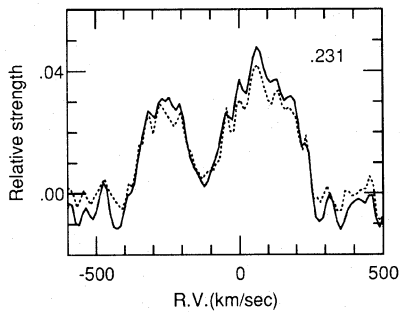


FIG. 5. A comparison of the BF (solid line) based on the template HD 102870 with the one (dotted line) based on HD 171232 for one of our spectra. Because of the better match of the spectral type between HD 171232 (G8III) and AH Vir (G8V), the zero point of the BF based on HD 171232 was defined better than that of the BF based on HD 102870 (F9V). The scaling factor of the former to the theoretical BF is also closer to unity than that of the latter (see text). However, we used HD 102870 as our template because of the higher S/N of its spectrum.

radial velocity analysis (Sec. 4), and $i$ fixed from the light curve solution (Sec. *5.1*) we can attempt to determine the two most elusive parameters, $f$ and $X$.

In order to find the best fitting pairs $(f, X)$ from the observational BF's, we used a grid of theoretical broadening profiles generated by means of the same program as the one used for the light curve solution. For each combination of $f$ and $X$, we calculated the global quality-of-fit measure $Q=\Sigma(\text{O–C})^2/\Sigma n$, with summation extended over all non-zero valued points of the theoretical BF's at all 23 phases. All the other adopted parameters were the same as for the light curve solution except that the limb-darkening and emergent intensity input data were interpolated into the central wavelength of 5000 Å of the spectroscopic observations.

As was described in Sec. 3, two standard stars were used for the BF determinations. They were HD 102870 (F9V) and HD 171232 (G8III). The former was observed with the high S/N of about 250 but its spectrum is a poor match for the AH Vir spectrum.[3] The latter star could provide a better template but it was observed with the low S/N of about 100. Since both cases do not offer an ideal template for the AH Vir spectra, we decided to perform the $(f, X)$ determinations with a simultaneous linear scaling of the BF by a common (for all phases) zero point and a common scale factor. This should, to first order, compensate for the spectral mismatch. We found that the BF's obtained using HD 102870 required a small negative zero-point shift and had larger amplitudes than the theoretically predicted ones. However, they did lead to reliable determinations of $(f, X)$ as given in the fourth column of Table 3. On the contrary, the spectrum of HD 171232 used as the BF restoration template apparently matched the AH Vir spectra much better because the zero-point shift was very small and the scale was close to unity. However, because of the lower S/N of the spectrum of the star, no reliable information about the degree-of-contact $f$ could be derived from the corresponding BF's. The solutions drifted to a large $f$ of about 0.75 and the value of $X$ was physically unacceptable. We could determine $X$ by fixing $f$ at the value derived from the BF's based on HD 102078 but we consider these solutions to be uncertain and unreliable. These problems of the template selection are illustrated graphically in Fig. 5. This figure shows a detailed comparison of the BF results for both template stars for one phase close to the orbital quadrature.

The best fitting values of $(f, X)$ and their uncertainties were obtained by analyzing the shapes and widths of minima of the function $Q$ (defined above) in the space of parameters $(f, X)$. The uncertainties are expressed as mean standard errors and were evaluated by taking into account the widening of the minimum for two parameters, as described in Chap. 14.5 of Press *et al.* (1986). The final results are given separately for both templates in the last two columns of Table 3. We note that values of the degree of contact are in close agreement between the light curve and BF solutions, but the values of the temperature excess are different (in that the spectral results obtained at about

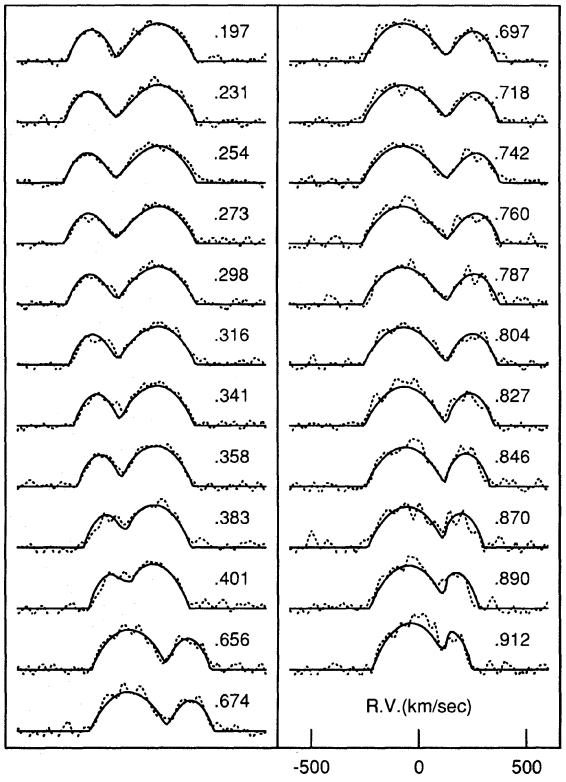


FIG. 6. An overall comparison of the observational BF's (dotted lines), based on the template of HD 102870, with the theoretical ones (solid lines). The orbital phases are given for each of the profiles.

TABLE 5. Absolute parameters of AH Vir.

| | |
|---|---|
| $a$ $(R_\odot)$ | $2.796 \pm 0.017$ |
| $i$ (°) | $85.2 \pm 1.2$ |
| $q$ $(m_2/m_1)$ | $0.303 \pm 0.006$ |
| $M_1$ $(M_\odot)$ | $1.360 \pm 0.024$ |
| $M_2$ $(M_\odot)$ | $0.412 \pm 0.010$ |
| $R_1$ $(R_\odot)$ | $1.397 \pm 0.008$ |
| $R_2$ $(R_\odot)$ | $0.826 \pm 0.005$ |
| $L$ $(L_\odot)$ | $1.87 \pm 0.28$ |
| $L_1(corr)$ $(L_\odot)$ | $1.86 \pm 0.28$ |
| $M_{bol}$ $(mag.)$ | $4.07 \pm 0.16$ |
| $M_v$ $(mag.)$ | $4.25 \pm 0.16$ |
| $d$ $(pc)$ | $94 \pm 7$ |

Comments:

* Assumed: $T_{eff} = 5300 \pm 200$, Sp.type = G8 ± 2V, V = 9.12, $E_{B-V} = 0$.

[3]The spectral type of both components of AH Vir would be basically identical within the strict contact model. Our parametrization of the higher surface brightness of the secondary in terms of the parameter $X$ leads to a temperature excess of about 350 K which, in principle, should be visible as a difference in spectral type of about two subtypes. That we do not see this difference confirms that the parameter $X$ represents actually the differential dark-spot coverage of both components.

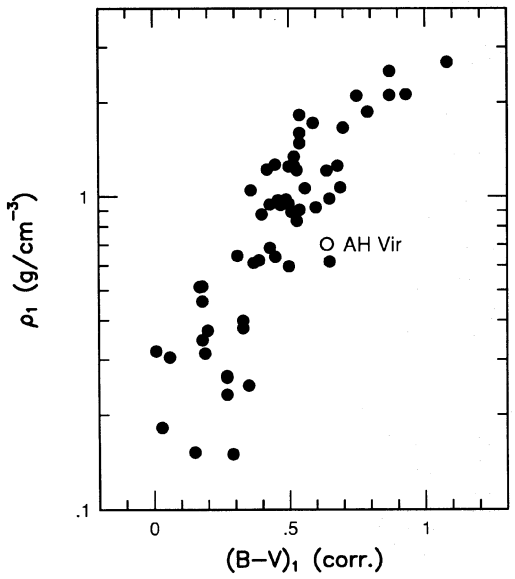


FIG. 7. Mean densities of the primary components of W UMa-type system and their colors, corrected for the effects of the energy transfer, as tabulated by Mochnacki (1985). The new position of AH Vir is marked by an open circle. Its neighbor is OO Aquilae. The mean density for AH Vir is identical whether we use the Mochnacki's approach or determine it directly from the spectroscopically derived values of the mass and radius.

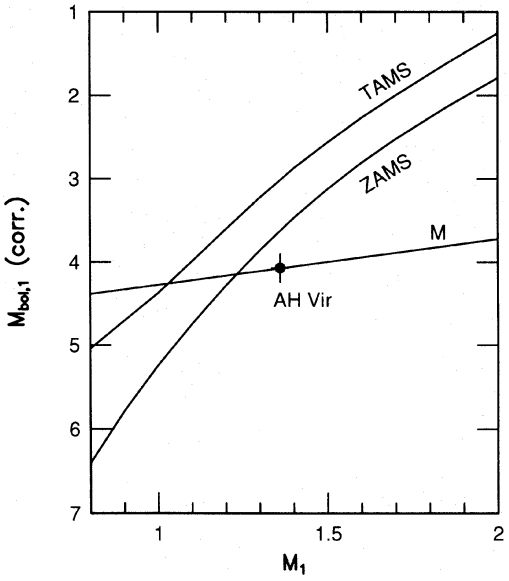


FIG. 8. The bolometric magntiude of the primary, corrected for the energy transfer and the mass of the primary resulting from our new spectroscopic orbit of AH Vir are shown by a filled circle. The line marked M gives the relation which can be obtained using Mochnacki's (1981) simple approach based only on the period, color, mass ratio, and degree of contact. The ZAMS and TAMS lines come from the VandenBerg (1985) model calculations for the solar abundance. Since metallicity of AH Vir is unknown, we note that the ZAMS line for the abundance reduced by the factor of ten is almost coincident with the TAMS line shown here.

5000 Å agree better with those from the $B$ light curve). This is again presumably because the photometry and spectroscopy of AH Vir were made at different epochs, which were probably characterized by quite different spot distributions.

Figure 6 gives a collection of all observational determinations of the broadening functions. They were all based on HD 102870. The dotted lines give the observed BF's, whereas the theoretical ones are shown by continuous lines. The agreement between the observational and theoretical BF's is very good and no obvious deviations from the contact model are seen at any orbital phase.

## 6. ABSOLUTE DIMENSIONS AND PHYSICAL PARAMETERS

We derived the absolute elements of AH Vir by performing a "stretch and shift" broadening function fit for the best estimates of $K_1+K_2$ and $V_0$ using the final set of the geometrical elements, as given in the last line of Table 4. This solution is given in the last column of Table 2. The absolute parameters obtained by combining these results are listed in Table 5. The radii were derived by combining the component separation with the relative volume radii of the components, $r_1=0.500$ and $r_2=0.295$, computed for the adopted values of $q=0.303$, $f=0.230$. To estimate the uncertainty in the system luminosity, it was assumed that $T_1=5300$ K had an uncertainty of 200 K in accordance with the uncertainty in the spectral classification (G8±2 V, see Sec. 2). The luminosity and absolute bolometric magnitude were derived by adopting $T_{\text{eff}\odot}=5780$ K and $M_{\text{bol}\odot}=4^{\text{m}}.75$, with the bolometric correction taken from Popper (1980). The luminosity of the system was computed by multiplying the area of the system in relative units (which depends only on $q$ and $f$) by the square of the orbital separation and by $\sigma T_{\text{eff}}^4$. Note that with $q=0.303$, the primary component provides 99.5% of the total systemic luminosity (assuming the nuclear dependence $L_2/L_1 \propto q^{4.4}$).

The well-determined set of the absolute parameters of AH Vir not only offers insight into the structure of this unique system but also permits a consistency check on the simple but powerful approach of Mochnacki (1981, 1985) for the cases when the spectroscopic data are not available. As can be seen in Fig. 7, which is copied from Fig. 5 of Mochnacki (1985), but with the new location of AH Vir resulting from the new values of $q$ and $f$, the system seems to belong to the group of OO Aquilae contact with systems which deviate from most of the W UMa systems by having abnormally low densities for their effective temperatures. Since $q$ is now reduced relative to the older value, the primary component is relatively larger and its density is lower than estimated before. The mean density, 0.70 g/cm$^3$, approximately corresponds to that of a Main-Sequence (MS) 1.36$\mathcal{M}_\odot$ star.

It is interesting to compare the mean densities of primary components of AH Vir and OO Aql since both sys-

tems have unusual locations in Fig. 7. Apparently, both systems are bigger and cooler than most of the contact systems. However, the primary of AH Vir is *not* oversized relative to the MS mass–radius relation as in OO Aql (Hrivnak 1989): its radius, 1.40 $R_\odot$, roughly corresponds to a 1.36$\mathcal{M}_\odot$, F5V star. It is another matter that the secondary is oversized. This is a common situation in contact binaries which can be explained by the energy transfer. But what is clearly unusual with AH Vir is its low luminosity, apparently resulting from the low effective temperature of the system.

We compare our spectroscopic determination of the primary mass, 1.36$\mathcal{M}_\odot$, and the total luminosity of AH Vir, 1.9 $L_\odot$, with the model calculations in Fig. 8. The lines give the theoretical Zero-Age and Terminal-Age Main Sequences (ZAMS) and (TAMS) from VandenBerg (1985) for the solar abundance. In addition, we give another mass–luminosity relation (the "Kepler relation") which AH Vir must obey following the simple approach of Mochnacki (1981; Sec. V). This simple approach permits finding the (shallow) dependence of the energy-transfer corrected $M_{\rm bol}$ on the primary mass on the basis of the photometric data. This line is marked M in Fig. 8.

Apparently, AH Vir is underluminous even when compared with the ZAMS, which is fainter than the observational MS. The low luminosity of AH Vir is a direct consequence of its low effective temperature, which remains abnormally low even when corrected for the energy transfer to the secondary component. This correction, $\Delta \simeq 400$ K, would produce $T_1(\mathrm{corr}) \simeq 5700$, $sp \simeq$ G2 V, far below what could be expected from a 1.36 $\mathcal{M}_\odot$ star apparently obeying the MS mass–radius relation. Thus, AH Vir and OO Aql, in spite of sharing low densities and low effective temperatures, are *not* similar in their internal structure because AH Vir does not have an oversized primary—for its mass—which is the clearest sign of being evolved. On the other hand, it would be very difficult to explain peculiarities of AH Vir without invoking evolution; otherwise the system—most probably—would not be in contact.

## 7. SPACE MOTIONS

The distance to AH Vir can be determined by combining the absolute magnitude of the system, $M_v = 4.25$, with the apparent magnitude. The visual apparent magnitude is $9^{\rm m}.12$ with an uncertainty of $0^{\rm m}.01$ at the phase close to the light maximum (Rucinski & Kaluzny 1981). The galactic coordinates of AH Vir are: $l = 271^\circ.5$ and $b = 72^\circ.4$. At the position there is no extinction according to the reddening map of Burstein & Heiles (1982). Combining these data, we obtain the distance to the star of $94 \pm 7$ pc. This estimate is in very good agreement with that of 92 pc derived by Rucinski & Kaluzny (1981) and is smaller than the 127 pc found by Guinan & Bradstreet (1988).

On the basis of the estimate of the distance, the space motion of AH Vir was derived by combining the SAO Catalogue proper motions $\mu_\alpha \cos(\delta) = 0''.022$/yr and $\mu_\delta = -0''.111$/yr with the systemic velocity of 8.1 km/s. The three components of the spatial velocity relative to the Sun are as follows: $U = 33.1 \pm 6.1$ km/s toward the galactic center; $V = -38.9 \pm 5.6$ km/s in the direction of galactic rotation; and $W = -4.1 \pm 2.0$ km/s toward the north galactic pole. The total spatial velocity of the system is then about 50 km/s relative to local standard of rest if the standard solar motion (+10.4, +15.0, +7.3 km/s) is adopted. Guinan & Bradstreet (1987) derived a value of 67 km/s for the total spatial velocity because they used a larger distance.

We cannot add more to the suggestion of Eggen (1965, 1969, 1983) that AH Vir is a member of the Wolf 630 moving group but we note that his space velocities were smaller than derived here [and even more so relative to Guinan & Bradstreet (1987)] as he apparently adopted the distance 76–81 pc. We agree with Eggen and with Guinan and Bradstreet that, according to the kinematic data, AH Vir belongs to the old disk population.

## 8. CONCLUSIONS

We have redetermined the spectroscopic orbit of AH Vir on the basis of new spectra which were processed using the method of the broadening functions. This method permits extraction of the radial velocity data in an optimal way from the whole available length of the spectrum, and is clearly superior to the cross-correlation function because it is insensitive to the presence of broad spectral features in the spectrum.

Our new result for the mass ratio, $q = 0.30$, is smaller than the Chang (1948) value which led Mochnacki (1981) to infer that AH Vir has more angular momentum than ordinary MS objects and that it originated from a detached binary system. We note that adoption of a smaller mass ratio leads to an increase in the relative size of the primary and hence to its lower mean density.

The observed radius of the primary is surprisingly close to the MS value for 1.36 $\mathcal{M}_\odot$. Thus, the mean density and dimensions of the primary are close to that of an F5 MS star. But the *total systemic* luminosity is $1.9 \pm 0.3$ $L_\odot$ which is much lower than for a MS F5 star (contribution from the secondary should be $\simeq 0.5\%$) on account of the very low effective temperature of the system. The expected luminosity for such a star would be $3.4 < L/L_\odot < 4.7$ depending on the exponent $\alpha$ in $L \propto \mathcal{M}^\alpha$, for $4 < \alpha < 5$. A spectrophotometric determination of the effective temperature of AH Vir would be certainly useful at this stage but the data at hand show that the temperature is low. The colors $B-V \simeq 0.76$, $b-y \simeq 0.48$ (Rucinski & Kaluzny 1981, Table 1) and the DDO photometry (Hilditch 1981) are fully consistent with literature spectral classifications of G8 to K0, for $E(B-V) \leqslant 0.02$.

We should note that without the new data on the mass of the system we would have a very different picture of the system as its low temperature still places AH Vir *above* the MS on the color–magnitude diagram. But this position is entirely inconsistent with the large masses of components.

In spite of sharing some unusual properties with OO Aql, such as the low mean density and low effective temperature (for its period), AH Vir is not similar to OO Aql.

It is a relatively massive system having dimensions and a period more or less appropriate for its mass. It does not show clear signs of being evolved except for its abnormally low effective temperature. The current evidence does not obviously require that AH Vir be a contact descendant of a detached binary. If the low effective temperature is due to photospheric spots, we would have to explain why a basically normal G2-type contact system has so extensive spot coverage that its spectral type is pushed down to K0.

We should note that AH Vir is lengthening its orbital period with a relatively short characteristic time scale $d \ln P/dt \simeq 1.7 \times 10^6$ yr (Demircan *et al.* 1991), which indicates a moderately strong mass transfer. As illustrated by model calculations of Webbink (1976), a strong mass flow may lead to a substantial drop in systemic luminosity. However, for AH Vir, the sign of the flow suggests transfer from the less massive to the more massive component which, on account of the gravitational terms, should result actually in an increase of brightness. On the other hand, the Roche lobe of the primary must be expanding at the same time, which may lead to a luminosity sink. All these processes of the mass transfer and stability adjustment are expected to take place in somewhat similar thermal time scales. Possibly, AH Vir is seen by us in a stage when no luminosity equilibrium has been achieved.

We would like to thank Jun Shi for help in determination of the broadening functions and Dr. Nancy Evans for careful reading of the manuscript and for useful comments. Special thanks are due to Dr. Stefan Mochnacki for his comments on the manuscript, for useful discussions and for suggesting the name "red straggler" to describe the unusual properties of AH Vir. Dr. David Holmgren and Dr. Bruce Hrivnak carefully read the manuscript and suggested numerous improvements which are acknowledged here with gratitude. This work was supported by an operating grant from the Natural Sciences and Engineering Council of Canada to S. M. R.

## REFERENCES

Al-Naimiy, H. M. 1978 Ap&SS, 53, 181
Bakos, G. A. 1977, Bull. Astr. Inst. Czech., 28, 157
Barden, S. C. 1984, PhD thesis, Pennsylvania State University
Barden, S. C. 1985, ApJ, 295, 162
Binnendijk, L. 1960, AJ, 65, 358
Binnendijk, L. 1984, PASP, 96, 646
Burstein, D., & Heiles, C. 1982, AJ, 87, 1165
Chang, Y. C. 1948, ApJ, 107, 96
Demircan, O., Derman, E., & Akalin, A. 1991, AJ, 101, 201
Eaton, J. A., Wu, C. -C, & Rucinski, S. M. 1980, ApJ, 239, 919
Eggen, O. J. 1965, The Observatory, 85, 191
Eggen, O. J. 1969, PASP, 81, 553
Eggen, O. J. 1983, AJ, 88, 813
Guinan, E. F. & Bradstreet, D. H. 1988, in Formation and Evolution of Low Mass Stars, edited by A. K. Dupree and M. T. V. T. Lago (Kluwer, Dordrecht), p. 345
Guthnick, P., & Prager, R. 1929, Beob. Zirk. No. 13, 32
Hill, G. 1991, private communication
Hill, G., Hilditch, R. W., Younger, F., & Fisher, W. A., 1975, MNRAS, 79, 131
Hilditch, R. W. 1981b, MNRAS, 196, 305
Hrivnak, B. J. 1989, ApJ, 340, 458
Jabbar, S. R., & Kopal, Z. 1983, Ap&SS, 92, 99
Kaluzny, J. 1984, AcA, 34, 217
Lucy, L. B. 1967, Z. Astrophysik, 65, 89
Lucy, L. B. 1973, Ap&SS, 22, 381
Mochnacki, S. W. 1981, ApJ, 245, 650
Mochnacki, S. W. 1985, in Interacting Binaries, edited by P. P. Eggleton and J. E. Pringle (Reidel, Dordrecht), p. 51
Mochnacki, S.W., & Doughty, N. A. 1972, MNRAS, 156, 51
Mullan, D. J. 1975, ApJ, 198, 568
Niarchos, P. G. 1983, A&AS, 53, 13
Press, W. H., Flannery, B. P., Teukolsky, S. A., & Vetterling, W. T. 1986, Numerical Recipes: The Art of Scientific Computing (Cambridge University Press, Cambridge)
Popper, D. M. 1980, ARA&A, 18, 115
Rucinski, S. M. 1969, AcA, 19, 245
Rucinski, S. M. 1974, AcA, 24, 119
Rucinski, S. M. 1976a, PASP, 88, 777
Rucinski, S. M. 1976b, AcA, 26, 227
Rucinski, S. M. 1985, MNRAS, 215, 615
Rucinski, S. M. 1992a, AJ, 103, 960
Rucinski, S. M. 1992b, AJ, 104, 1968 (Paper I)
Rucinski, S. M., & Kaluzny, J. 1981, AcA, 31, 409
VandenBerg, D. A. 1985, ApJS, 58, 711
Webbink, R. F. 1976, ApJS, 32, 583
Wilson, R. E. 1979, ApJ, 234, 1054
Wilson, R. E., & Sofia, S. 1976, ApJ, 203, 182